Effects of Congo Red on Aβ_{1-40} Fibril Formation Process and Morphology

Partha Pratim Bose,[†] Urmimala Chatterjee,[§] Ling Xie,[‡] Jan Johansson,[§] Emmanuelle Göthelid,*[,‡] and Per I Arvidsson*[,†,∥]

[†]Department of Biochemistry and Organic Chemistry, Uppsala University, Box 576, S-75123 Uppsala, Sweden, [§]Department of Anatomy, Physiology and Biochemistry, Swedish University of Agricultural Sciences, The Biomedical Center, Box 575, S-75123 Uppsala, Sweden, [‡]Department of Physics and Materials Science, Uppsala University, Box 530, 751 21 Uppsala, Sweden, and [∥]Discovery CNS & Pain Control, AstraZeneca R&D Södertälje, S-151 85 Södertälje, Sweden

Abstract

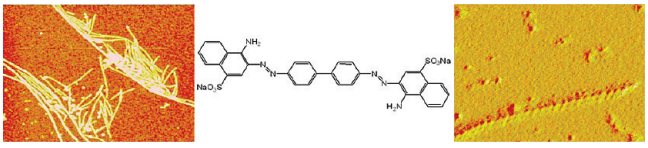

Alzheimer's disease (AD), an age-related neurodegenerative disorder, is the most common form of dementia, and the seventh-leading cause of death in the United States. Current treatments offer only symptomatic relief; thus, there is a great need for new treatments with disease-modifying potential. One pathological hallmark of AD is so-called senile plaques, mainly made up of β-sheet-rich assemblies of 40- or 42-residue amyloid β-peptides (Aβ). Hence, inhibition of Aβ aggregation is actively explored as an option to prevent or treat AD. Congo red (CR) has been widely used as a model antiamyloid agent to prevent Aβ aggregation. Herein, we report detailed morphological studies on the effect of CR as an antiamyloid agent, by circular dichroism spectroscopy, photo-induced cross-linking reactions, and atomic force microscopy. We also demonstrate the effect of CR on a preaggregated sample of Aβ_{1-40}. Our result suggests that Aβ_{1-40} follows a different path for aggregation in the presence of CR.

Keywords: Alzheimer's disease, atomic force microscopy, Congo red, amyloid, oligomers, fibrils, aggregates, amyloid β-peptide

The aggregation of proteins into amyloid fibers is associated with a growing list of diseases, including Alzheimer's and the prion diseases (*1*−*3*). Amyloid formation is a highly complex process, in which proteins with distinct biological properties lose their native structures and become aggregated into insoluble deposits (*4*). In Alzheimer's disease (AD) (*5*), a 40- or 42-residue peptide, popularly known as amyloid β-peptide (Aβ), assembles into long, unbranched fibers after folding through a β-sheet-rich conformation. These fibrils in turn aggregate into amyloid plaques, which were for many years considered to be the toxic pathological hallmark of AD; however, during the last years, a growing number of reports suggest that the most toxic agent of Aβ is nonfibrillar and oligomeric in nature. The evolution of highly toxic amyloid-derived diffusible ligands (*6*) and other aggregates (*7*−*9*), even in the presence of biological lipids (*10*), are increasing the list of toxic species. Recently, it has been found that resveratrol, a polyphenolic from red wine, attenuates oligomeric cytotoxicity of Aβ_{1-42} but does not prevent oligomer formation (*11*). Such findings render *in vitro* characterization of Aβ aggregation an important endeavor. It is known that a high degree of β-sheet structure content is a necessary condition for amyloid toxicity, but it may not be a sufficient proviso, as demonstrated by the recent isolation of β-sheet-rich nontoxic fibrillar aggregates upon treatment of Aβ with sulfated polysaccharide inhibitors (*12*) and by another report where methylene blue was shown to accelerate formation of β-sheet fibrils and thereby lower the concentration of toxic oligomers (*13*). Thus, a thorough characterization of the morphologically distinct species that evolve upon incubation of Aβ with various antiamyloidogenic compounds may help to rationalize how different inhibitors operate and lead to an increased knowledge for the design of new ones (*14*−*16*).

At present, there are no approved therapies that target amyloid formation directly, but many organic molecules have been shown to inhibit fibrillation *in vitro*, and thus represent an increasing list of proposed antiamyloid lead compounds. Congo red (CR) (*17*), a well-known histological stain, is widely used to demonstrate the presence of amyloidogenic deposits in tissues. Burgevin et al. have demonstrated that CR inhibited the aggregation of amyloid β-peptide and protected hippocampal neuron cultures of rat from Aβ-associated toxicities (*18*). Congo red has also been found to block

Received Date: December 18, 2009
Accepted Date: January 22, 2010
Published on Web Date: February 03, 2010

DOI: 10.1021/cn900041x | *ACS Chem. Neurosci.* (2010), *1*, 315–324

the aggregation of $A\beta_{1-40}$ in human macrophage culture (*19*). From a study in a *Drosophila melanogaster* model expressing Aβ, (*20*) it was established that CR ensured protection against Aβ-aggregation even under *in vivo* conditions, as feeding flies with 5% w/v CR resulted in marked survival prolongation and reduction in the amount of $A\beta_{1-42}$ aggregates in the brain (*21*). Furthermore, Chauhan et al. recently showed that CR inhibits the undesired binding of fibrillar Aβ with proteases such as trypsin, insulysin, and neprilysin. These enzymes, important for the proteolytic clearance of soluble Aβ aggregates, were inactivated by interaction with fibrillar Aβ. CR's interaction with the fibrillar form of Aβ shielded the interaction between the catabolic enzymes and the latter, thus rendering the enzymes free for their catabolizing activity on the toxic soluble form of Aβ (*22*).

These prominent examples of the antiamyloidogenic properties of CR have sparked an interest in developing new congeners during the last couple of years (*17*, *23*, *24*). Despite the interest of CR and its use as an antiamyloid agent, to the best of our knowledge, there are no reports on the morphological details of the various Aβ aggregates formed at different time points under treatment with CR. Keeping this in mind, we set out to study the effect of CR on the $A\beta_{1-40}$ fibrillation process and on various preformed $A\beta_{1-40}$ aggregates to a higher detail. In this regard we used atomic force microscopy (AFM) to study aggregated structures at different phases of the aggregation process of $A\beta_{1-40}$ in presence of CR (*20*). We also studied the effect of CR on the secondary structural feature of $A\beta_{1-40}$ during the early stage of the fibrillation process by circular dichroism spectroscopy (CD). Moreover, photo-induced cross-linking of unmodified protein (PICUP) (*25*, *26*) followed by SDS−PAGE was employed to assess the oligomeric nature of various aggregates of $A\beta_{1-40}$ seen by AFM at different time points after CR treatment.

Results and Discussion

Effect of CR Addition on the Fibrillation Process of $A\beta_{1-40}$

CD spectroscopy has been used to study the kinetics of secondary structure changes (*27*−*29*). A general feature emerging from biophysical studies suggests that Aβ exists in a "natively unfolded" conformation and undergoes nucleation-dependent self-assembly. It is reported that Aβ forms oligomeric "paranuclear" units, which self-assemble to form beaded protofibrils, which in turn aggregate to form fibrils, eventually leading to plaque formation (*4*). Throughout this self-assembly process β-sheet structures become more and more dominant (*30*). Here, we employed CD spectroscopy to determine the effect of CR on the structural change of $A\beta_{1-40}$ during the aggregation process. At the starting point, $A\beta_{1-40}$ was in a predominantly unordered conformation as described in the literature. With time, an increased β-structural content was observed, that is, the characteristic kinetic feature of aggregation (Figure 1a) (*27*). Comparing the spectral evolution over time, we saw that addition of CR did not significantly retard the adoption of β-structure by Aβ (Figure 1a,b). Aβ treated with CR reached a conformational state with a considerable amount of β-structure at 2 h, and at the same time point, Aβ also possessed β-structure but in a comparably smaller amount. Thus, it appears CR is capable of catalyzing Aβ's conformational change from random coil to β-sheet. We also carried out the CD experiments with various ratios of concentrations of $A\beta_{1-40}$; the accelerating effect of CR on the formation of β-sheet by $A\beta_{1-40}$ was evident in the whole concentration range studied ($A\beta_{1-40}$/CR 1:1 to 1:10, Supporting Information, Figure S1). The β-sheet formation by $A\beta_{1-40}$ in presence of CR also lacked the presence of any "lag phase" as observed in the CD of untreated $A\beta_{1-40}$ sample (Supporting Information, Figure S1d). These results suggest that the addition of CR may have triggered another mechanism of aggregation of Aβ different from its classical nucleation-dependent one, which is characterized by an initial "lag phase" during β-sheet formation (*4*). Because our CD experiments with varied concentrations of CR did not show much concentration dependence, we maintained a concentration ratio of 1:5 ($A\beta_{1-40}$/CR) for all our subsequent studies. It has previously been reported that CR stabilized the monomers of Aβ, and eventually it was postulated that the *in vitro* oligomerization, which follows shortly after dissolution of monomer in physiological buffer, might have been prevented upon CR treatment (*31*). Our result suggests that CR does not prevent the conformational conversion of Aβ to form substantial β-structures; instead it favors its formation by a kinetically accelerated pathway. These findings gave us the impetus to study the outcome of Aβ aggregation upon CR treatment for longer kinetic time points, that is, over days, and to study the fate of previously claimed CR-stabilized Aβ monomers during the aggregation process.

Photo-induced cross-linking of unmodified protein (PICUP) has been used to detect the SDS-unstable early oligomers of Aβ by converting them into SDS-stable, covalently linked oligomers using a photochemical reaction (*25*, *26*). PICUP experiments have been a popular approach to visualize the presence of lower order oligomers of Aβ as SDS-stable adducts. Recently, Ono et al. successfully used PICUP in establishing the activity of their proposed inhibitors against Aβ aggregation by comparing the oligomeric distribution pattern of Aβ

DOI: 10.1021/cn900041x | *ACS Chem. Neurosci.* (2010), *1*, 315–324

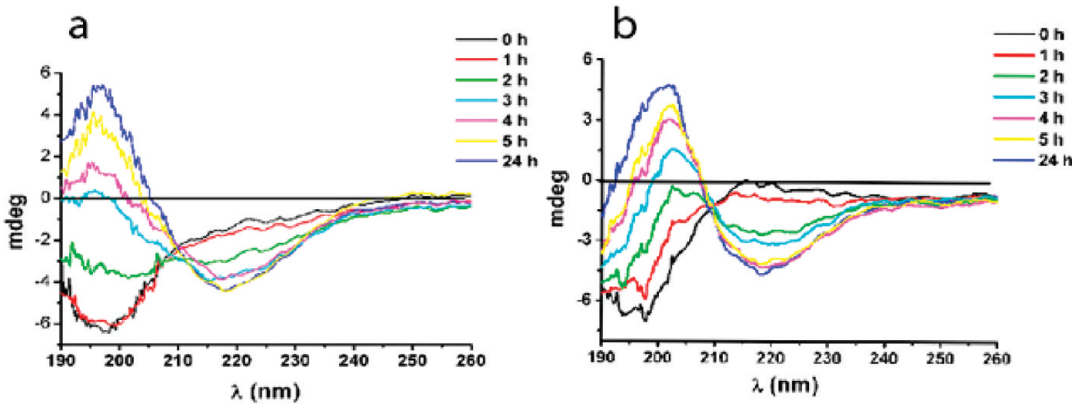

Figure 1. Circular dichroism spectra of (a) 20 μM Aβ_{1-40} and (b) 20 μM Aβ_{1-40} + 100 μM CR dissolved in phosphate buffer (pH 7.4) and incubated in 37 °C at different time points.

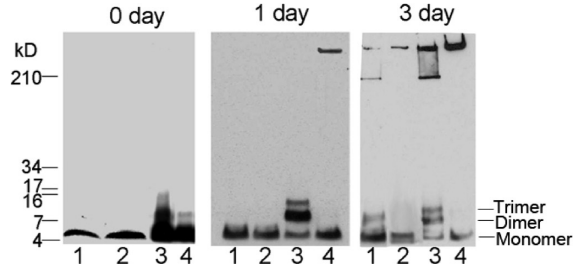

Figure 2. Photo-induced cross-linking of unmodified peptide (PICUP) was carried out for samples containing (lane 3) 20 μM Aβ_{1-40} alone and (lane 4) 20 μM Aβ_{1-40} + 100 μM CR. Lanes 1 and 2 represent control samples without employing PICUP. The experiments were performed with the samples incubated for 0, 1, and 3 days, respectively. Approximate molecular weight (in kD) as obtained by molecular weight marker is shown on the left-hand side.

with and without inhibitor treatment obtained after PICUP experiments (*29*).

It is evident from Figure 2 that at day 0, Aβ_{1-40} was initially present mostly in form of a heterogeneous mixture of monomer, dimer, and trimer. In the sample of Aβ_{1-40} without PICUP, only monomer band was observed initially because the smaller oligomers were not SDS-stable, but they became visible in the same sample when the PICUP process was performed (Figure 2) (*26*). In contrast, at day 0 in the CR-treated sample with PICUP, mostly monomers were present with no impression of smaller aggregates. This may be possible if CR molecules interacted with the initial small aggregates or oligomers of Aβ thus preventing their photochemical cross-linking. As a consequence, significantly different distribution of early aggregates was observed in the presence of CR than in the Aβ sample alone, where smaller aggregates like dimer or trimer were present in substantial amounts. Upon incubation for 1 day, the band corresponding to dimer and trimer in Aβ became prominent at the expense of monomer content. At the same point, CR-treated Aβ only showed monomer and larger aggregated species that could not enter the gel. Absence of lower order oligomers upon CR treatment indicated that the aggregation did not follow the normal process (*4*). After 3 days of incubation, Aβ had formed very large aggregates, which were arrested on top of the gel, along with prominent dimer and trimer band and a vanishingly faint expression of monomer. In the CR-treated sample however, monomer was minute, but the impression of larger aggregates became very prominent, still with the absence of dimer and trimer bands. These observations, along with CD data (Figure 1a,b and Supporting Information, Figure S1d), suggest that in the presence of CR, Aβ assembles faster or that it takes a pathway that seems to be different from the nucleation-dependent aggregation of forming higher order aggregates. The increasingly intensified band of higher order aggregates with time in the CR-treated sample also suggested that aggregation was still occurring.

To characterize the different pattern of aggregation observed in our previous experiments in greater detail, we have employed AFM, which has already proved its efficiency in studying the high-resolution structures of Aβ (*20*). Upon incubation at 37 °C and pH 7.4 (phosphate buffer) with agitation, Aβ_{1-40} self-assembles to form various types of aggregates. At the initial time of incubation, we found only very small entities devoid of any regular shape or size (Figure 3a). Upon incubation for consecutive days, more and more ordered structures were beginning to evolve. Shorter forms of fibrils, that is, protofibrils, were first detected after 2 days of incubation. After 3 days of incubation, fully grown fibrils were observed; these had varied widths, probably because the fibers were still within the process of maturation (Figure 3b). The morphology of the fibers was also varied with either smooth or nodular surface appearance. The distribution patterns of smooth and nodular fibers were distinctly different. The smooth fibers had mean height of 2.5 nm and mean width of 47.5 nm, whereas the nodular fiber had 4.15 and

DOI: 10.1021/cn900041x | *ACS Chem. Neurosci.* (2010), *1*, 315–324

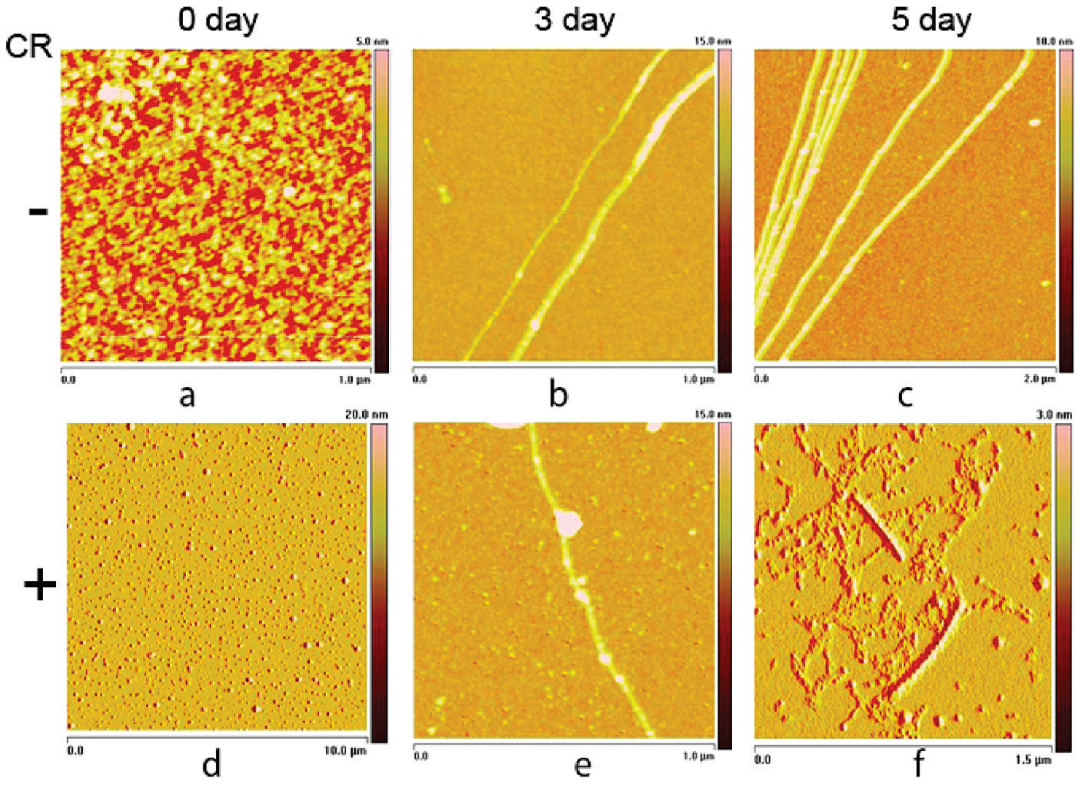

Figure 3. Atomic force microscopy (AFM) images of 20 μM Aβ_{1-40} in phosphate buffer (pH 7.4) at time (a) 0, (b) 3, and (c) 5 days after incubation at 37 °C and 20 μM Aβ_{1-40} treated with 100 μM CR in phosphate buffer (pH 7.4) at time (d) 0, (e) 3, and (f) 5 days after incubation at 37 °C.

83.5 nm, respectively (Supporting Information Figure S2). Longitudinal stacking of protofibrils along the length of individual fibrils was also well resolved as seen in Figure 4a−c. This convincingly established the process of building individual fibrils by assembly of protofibrillar units coaxially (*4*). After 5 days of incubation, the heights and widths of individual fibrils became more homogenously distributed (Figure 3c). Protofibrils and other very thin and long immature fibrillar structures were evident even after 5 days of incubation (Figure 5a).

Incubation of Aβ_{1-40} with CR proved to have an effect on the size and shape of initial aggregates. As seen in Figure 3d, in the presence of CR, the sizes and shapes of the Aβ aggregates at the initial time were mostly homogeneous (compared with Aβ_{1-40} alone in Figure 3a), and the distribution of globular structures found on the surface was seen to be repetitive (Figure 3d). Very recently, Shoichet et al. showed that the effectiveness of small molecule inhibitors of amyloidosis depended on their colloidal nature (*32*). According to their suggestion, CR inhibition also belonged to this category of inhibitors; thus, CR aggregates in solution to form micelle- or vesicle-like aggregates, which was found to inhibit model enzymes. The aggregation of CR was also characterized by dynamic light scattering (DLS) experiments (*33*). On the same line, the globular structures of Figure 3d could depict the presence of aggregates of CR (see Supporting Information, Figure S3), which either interact with the monomers or lower oligomers (and eventually disrupt the structural integrity of early oligomers) or accelerate the aggregation process in such a way that lower oligomers cease to get detected in the PICUP result at day 1 (Figure 2). Both of these mechanisms are supported by the result shown in Figure 2 (lane 4; day 1), because only monomer and larger aggregates are detected; comparison of the intensities from the monomer and larger aggregate bands at days 1 and 3 suggests that the interaction with monomers or lower oligomers precedes the formation of larger aggregates.

In our subsequent observation, the formation of fibrils of Aβ_{1-40}, even in the presence of CR, was clearly noticeable. Although the number of occurrences was extremely low, the fibrils appear as fully grown in length after 3 days of incubation (Figure 3e). The most striking difference was in the morphology of the treated fibrils after 5 days of incubation. The fibrils were shorter compared with the full-grown nontreated Aβ_{1-40} fibrils (Figure 3c,f and Figure 4a−f). The distribution of height and width of the fibers was entirely different from that of both types of fibers, nodular and smooth surfaced, observed in nontreated Aβ_{1-40} samples after 5 days of

DOI: 10.1021/cn900041x | *ACS Chem. Neurosci.* (2010), *1*, 315–324

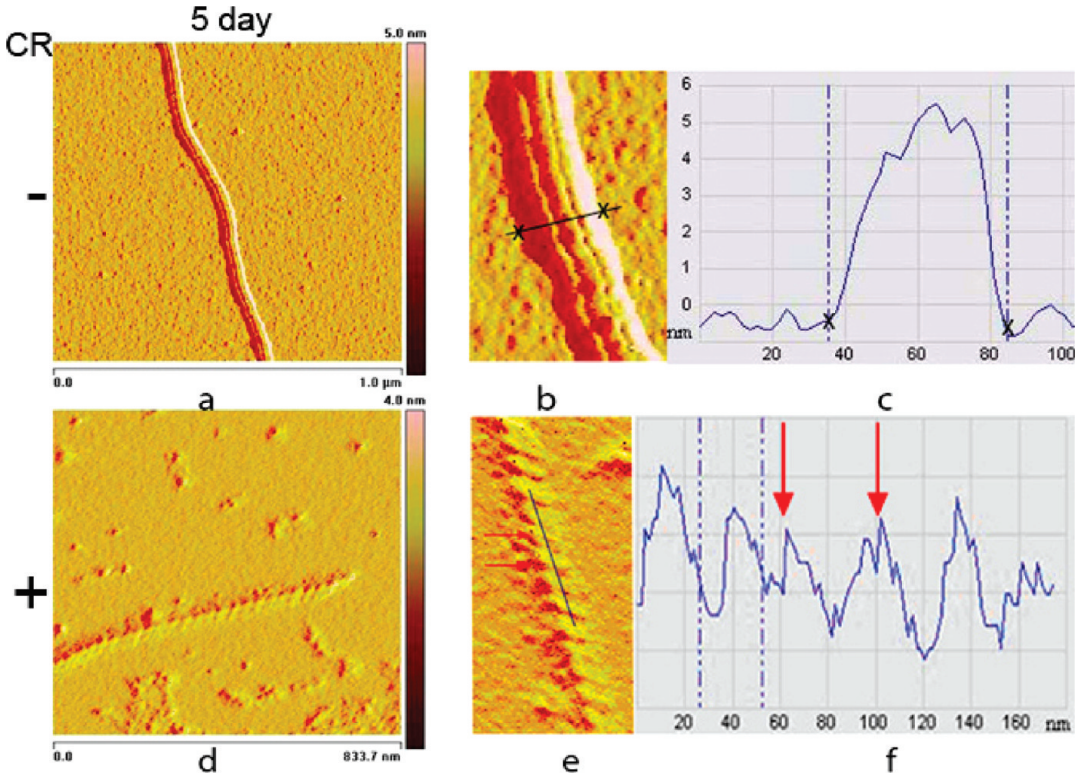

Figure 4. (a) Individual mature fibril of $A\beta_{1-40}$, (b) a part of the same fibril scanned at higher resolution, (c) transversal topographic profile of the same fibril scanned along the line in panel b, (d) fibrillar type aggregates at higher resolution as seen in the sample of $A\beta_{1-40}$ incubated with CR for 5 days, (e) part of the same fibril scanned at higher resolution, and (f) transversal topographic profile of the same fibril scanned along the line in panel e.

incubation (Supporting Information, Figures S2 and S4). The contours of the individual treated fibers were rough, and it seems that the small building blocks that were aligned to form the fibrils were entirely different from that of the nontreated fibers (Figure 4d−f and Supporting Information, Figure S5). The height scan of an individual nontreated fiber revealed a lateral stacking of intermediate units along the fiber axis (Figure 4b,c), whereas in case of the treated fibers, the height scan along the fibril axis on a high resolution individual fiber (Figure 4e,f) clearly shows spherical aggregates aligning together to form fibrillar structures (Supporting Information, Figure S5). This observation supports our conclusion that the formation of fibrils in presence of CR takes a different pathway, as compared to the native Aβ fibrillation process. More globular aggregates were observed in the presence of CR, compared with Aβ itself (Supporting Information, Figure S5). It seems that under CR treatment, Aβ prefers to follow the pathway of globular aggregate formation to fibrillation. As reported previously, the globular aggregates are evolved, probably by another exclusive mechanism, independent of the native fibrillation process (*7*). Our observations suggest that the presence of CR might trigger the pathway of formation of globular aggregates. The apparent similarity of morphology in Figure 3b,e can be explained by the fact that the native Aβ fibrillation process still occurs even in presence of CR, although the number of occurrence of fibers is negligibly small. As could be seen from our other experiment with CR and fully grown Aβ fiber from preaggregated Aβ sample (*vide infra*), CR binds and disaggregates the fully grown fibers (Figure 5f). A similar phenomenon is seen in Figure 3e, where a native-like fiber is formed but eventually it gets disaggregated and chopped by CR, leading to complete disappearance of such long fibers after 5 days. A close look at the sole fiber of Figure 3e would reveal the localization of CR aggregates along the length of the fiber.

Summing up our observations so far, we propose that CR arrests the monomers or early forming oligomers of Aβ and forms globular structures as seen in Figure 3d; which upon further aggregation produce either fibrillar or globular aggregates (seen in Supporting Information, Figure S5) by mutually exclusive pathways (hypothetically illustrated in Scheme 1). It has been observed from our CD experiments that during the early events of structural evolution, $A\beta_{1-40}$ forms β-sheet structure in an accelerated manner in presence of CR. This is in line with earlier literature, which ascribed accelerated adoption of β-sheet structure by the $A\beta_{1-40}$ backbone to the affinity of CR to interact with Aβ in a

DOI: 10.1021/cn900041x | *ACS Chem. Neurosci.* (2010), *1*, 315–324

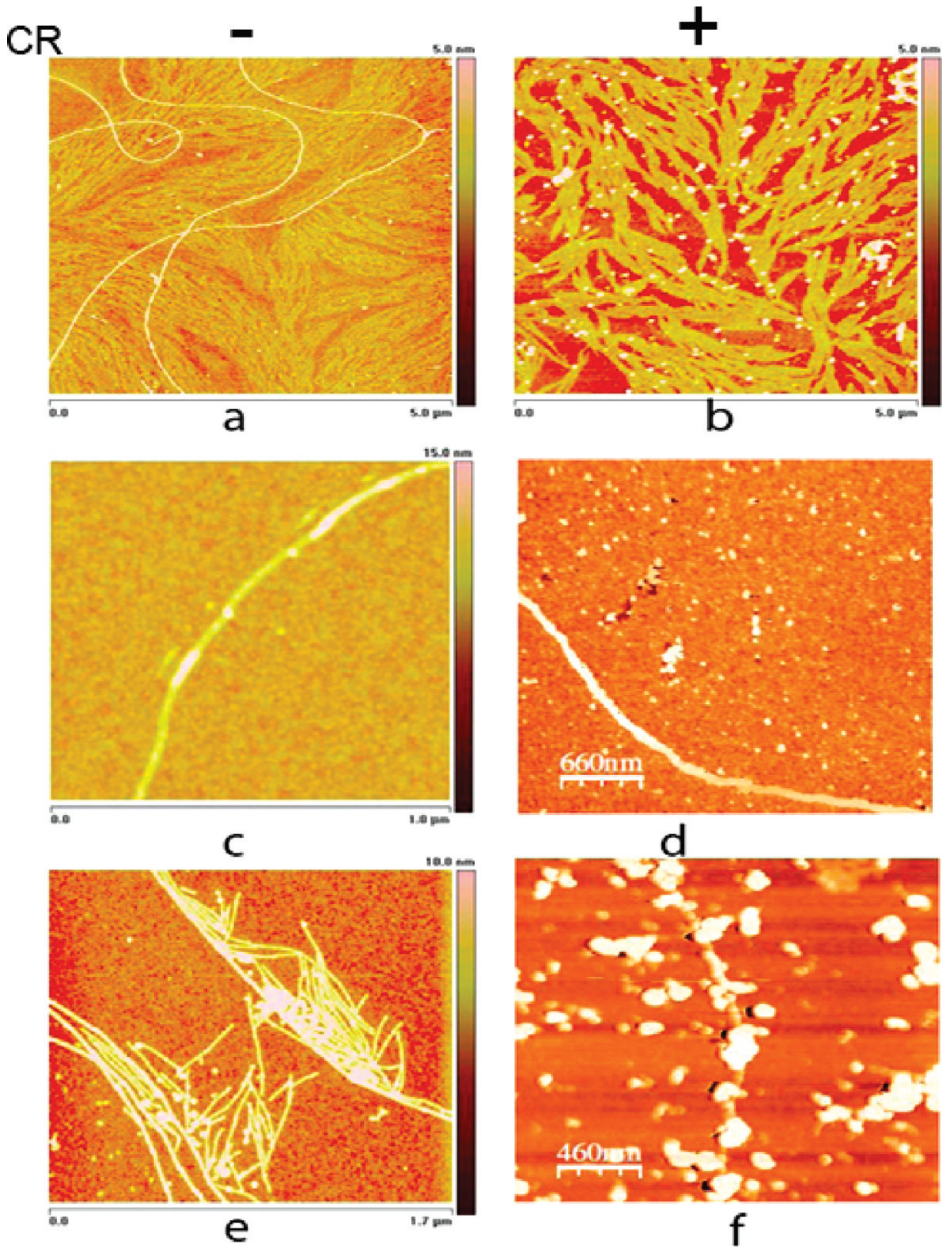

Figure 5. (a) Long mature fibril of Aβ1−40, finer fibrils, and other premature fibrillar aggregates as seen after 5 days incubation at 37 °C, (b) branched aggregates seen after treating 5-day mature Aβ1−40 fibrils with CR for 1 day, (c) individual matured fibril, (d) rarely seen individual mature fibril after treating 5-day mature Aβ1−40 fibrils with CR for 4 days, (e) plenty of fibrils and protofibrils of different lengths after 5 days of incubation of Aβ1−40, and (f) rarely observed full-length fibril after treating 5-day mature Aβ1−40 fibrils with CR for 5 days where aggregated CR was seen to be localized along the length of individual fibril.

β-strand conformation (*34*, *35*); CR might intercalate between early forming β-strand species to give them more stability, thus catalyzing the β-sheet formation.

Effect of CR Addition on Preformed Fibrillar Aggregates of Aβ

To study the effect of addition of CR on the 5-day matured Aβ aggregates formed by incubating at 37 °C, we performed an AFM study of the samples by adding CR and incubating it for yet another 5 days. It seemed that the addition of CR to the 5-day-old Aβ sample had manifold effects. The most prominent one was observed on the protofibrillar aggregates or other fine fibrillar structures that were seen previously (Figure 5a). After incubation with CR for 1 day, the finer protofibrils were thickened and merged together to form branched structures (compare Figure 5, panels a and b). At that point, the linearity of the finer fibrils was strikingly absent in the CR-treated sample. It may be due to the effect of the

DOI: 10.1021/cn900041x | *ACS Chem. Neurosci.* (2010), *1*, 315–324

Scheme 1. Hypothetical Model of A$\beta_{1\text{-}40}$ Aggregation in the Absence and Presence of CR[a]

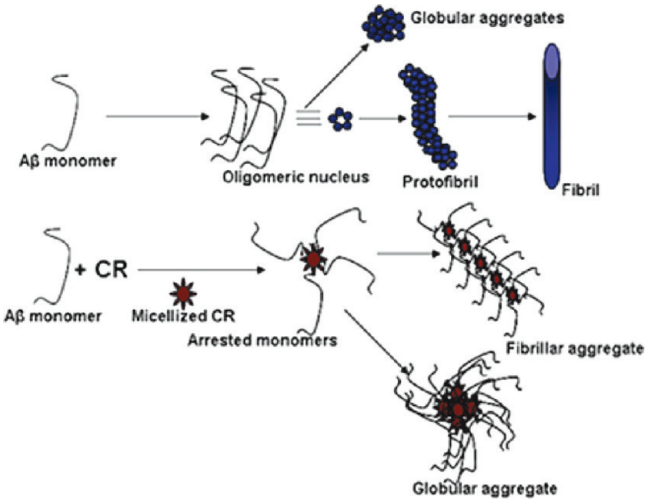

[a] Aβ_{1-40} monomers self-associate to form an oligomeric nucleus as an early event in the aggregation pathway prior to formation of protofibril and fibril. CR in aqueous solution forms colloidal aggregates, which upon incubation with non-aggregated Aβ_{1-40} arrest the monomers on its surface; the Aβ−CR conjugates thus formed further aggregate to produce aggregates of different shapes, for example, fibrillar or globular.

colloidal aggregation property of CR, which can arrest the floating fine fibrils to form these branched shaped ones (Figure 5b) (*32*). The mode and sites of binding of CR molecules along amyloid fibrils of Aβ_{1-40} has been previously determined for CR and analogs by Lockhart et al. (*36*, *37*). In the same line, Figure 5d shows the effect of CR addition on the fully grown fibril itself. These fibrils were no longer well resolved; it seemed that CR aggregates were coalescing along the length of the individual fibril (Figure 5f), which in turn may divide the long fibrils into shorter ones, thus supporting the fact that the number of occurrences of fibrils were vanishingly small after just 1 day of incubation of preformed fibrils with CR.

Many compounds have been reported to show antiamyloid activity in various *in vitro* and *in vivo* experiments, but a drug against Aβ toxicity in AD is yet to be identified. To date, many CR analogs, for example, BSB, X34, and X04, have been developed, although they eventually showed poor brain uptake (*38*−*40*). The CR-derived chrysamine G (CG) showed good BBB properties and alower toxicity level compared with CR (*35*), creating space for further development and characterization of CR congeners in search of new antiamyloids. Detailed structural studies of the mechanism of action of already available antiamyloids can help in future development and characterization of druggable modalities in AD. This study aimed to provide detailed morphological understanding of the mechanism of action of CR, which has been an archetypal antiamyloid for decades. From the results presented herein, we postulate that CR interacts with Aβ_{1-40} monomers or early forming oligomers and prevents formation of early aggregates or oligomeric paranucleus, which are considered to be the most toxic species in the amyloid cascade of Aβ (*41*−*45*). The hypothesis is that this interaction of CR with Aβ_{1-40} guides the peptide to a pathway of aggregation different from its classical nucleation-dependent one leading to fibril formation. By doing so, CR contributes to lowering the concentration of highly toxic smaller oligomers of Aβ generated in the early phase of amyloidogenesis. Fibrillation of Aβ_{1-40} in the presence of CR had not been previously reported; isolation of highly resolved fibrillar structures of Aβ in the presence of CR, although morphologically different from native fibrillar species of Aβ_{1-40}, demonstrates an alternative assembly process. Recent studies have suggested that therapeutic strategies aimed to reduce fibril formation may instead promote accumulation of smaller toxic oligomers. In this regard, it is of outmost importance to characterize the aggregates generated after treatment with antiamyloids. The methodologies presented here with CR would thus be highly beneficial for future characterization of Aβ aggregates in the presence of other inhibitors. At last, our endeavor to access the effect of CR on already aggregated species of Aβ_{1-40}, at a higher structural detail, being the first example of this kind, can well prove to be a vital step in developing inhibitors with specific actions on different aggregation phases of Aβ.

Methods

Materials

Amyloid β peptide (1−40), Aβ_{1-40}, was purchased from Bachem AG, Switzerland. Congo red was purchased from Sigma Aldrich.

Pretreatment of Aβ_{1-40}

To ensure aggregation free, low molecular weight (*46*) Aβ at the starting point of each experiment, Aβ was pretreated following the process adopted in the literature with slight modification (*12*). Briefly, 1 mg of Aβ was dissolved in 1 mL of TFA, and the TFA was removed under a gentle stream of argon. The peptide was then suspended in 1 mL of 1,1,1,3,3,3-hexafluoro-2-propanol (HFIP) and incubated at 37 °C for 1 h. The HFIP was evaporated under a stream of argon, and the resulting peptide film was dissolved in 2 mL of HFIP and divided into aliquots. HFIP was evaporated under argon, and the vials were kept for 3 h under 0.5 mbar to remove traces of HFIP. The aliquots were stored in an airtight vial at −20 °C. Immediately prior to use, the aliquots were dissolved to 200 μM in 20 mM NaOH, followed by brief sonication (*47*). This solution was diluted to 20 μM in 10 mM sodium phosphate buffer, pH 7.4, for all experiments.

For all experiments except CD, 20 μM of Aβ was incubated either separately or with addition of 100 μM CR at 37 °C with

DOI: 10.1021/cn900041x | *ACS Chem. Neurosci.* (2010), *1*, 315–324

shaking. For the CD experiments, 20 μM of Aβ was incubated either separately or with addition of 20, 100, and 200 μM CR at 37 °C with shaking. For determining the effect of CR on already aggregated Aβ_{1-40} samples, first 20 μM Aβ solution and was incubated for 5 days 37 °C with shaking. Then 100 μM CR solution was added to above solution and incubated under similar condition for another 5 days. For kinetic studies, samples were taken after specified time points and studied by the following experiments described below.

Atomic Force Microscopy

At specific time points, 2 μL aliquots of the incubated samples were dropped on a freshly cleaved mica surface and left for 2 min. Then the mica plate containing the drop of sample solution was washed gently with drops of deionized water and subsequently dried under dry argon flow. All the AFM measurements were performed in tapping mode using a Nanoscope 3a multimode instrument from VEECO. All the images were processed by WSxM software (*48*).

CD Spectroscopy

CD spectra were obtained using a Jasco-810-150S spectropolarimeter (Jasco, Japan). A quartz cell with 1 mm optical path was used. Spectra were recorded at 25 °C between 190 and 260 nm with a bandwidth of 1 nm, a 2 s response time, and a scan speed of 50 nm/min. Background spectra and when applicable, spectra of 20, 100, and 200 μM CR in phosphate buffer of pH 7.4 were subtracted. Each spectrum represents the average of three consecutive scans.

Photo-induced Cross-Linking of Unmodified Proteins (PICUP)

The photosystem required for performing PICUP experiments was constructed according to the description of the set up of Fancy and others (*25*, *26*) with some modifications. Irradiation was accomplished using a 200-W incandescent lamp and a 35-mm Pentax camera body with attached bellows. The bellows was attached to isolate the reaction tube from external light. The lamp was positioned 15 cm from the reaction tube at the open back of the camera. The irradiation time was 1 s and was controlled precisely using the camera shutter.

Photochemical Reaction. In a typical experiment, 1 μL of 1 mM Tris(2,2′-bipyridyl) dichlororuthenium(II) (Ru(Bpy), Sigma) and 1 μL of 20 mM ammonium persulfate, APS (Sigma) in buffer A (10 mM sodium phosphate, pH 7.4) were added to 18 μL aliquots taken at each time point. The mixture was irradiated, and the reaction was quenched immediately with 10 μL of Tricine sample buffer containing 5% β-mercaptoethanol.

Samples were analyzed by SDS−PAGE on 10−16% Tris−Tricine gel. Non-cross-linked Aβ with and without CR treatment was used as a control for each cross-linked peptide. After SDS−PAGE, the proteins from the gel were electroblotted (*49*) onto nitrocellulose membrane for 1 h at 100 mA and 40 V by using Tris−glycine buffer containing 25% methanol. The unoccupied sites of the membrane were blocked by incubation with 1% BSA in phosphate-buffered saline (PBS, pH 7.0) containing 0.05% Tween-20 (PBST) for 1 h at room temperature. The membrane was washed three times with PBST and incubated overnight with 6E10 antibody (1:5000). After the membrane was washed with PBST, it was again incubated for 1 h with ECL mouse anti-IgG antibody (1:5000). Next the membranes were washed again with PBST and incubated for 5 min with ECL solutions. The membrane was then developed in a PROTEC developer (Process technology, Germany).

Supporting Information Available

CD spectra at different ratios of CR/Aβ, distribution curves of occurrence versus height and width of Aβ nodular and smooth fibers, AFM of CR aggregates, distribution curves of occurrence versus height and width of Aβ fibers with and without CR, and AFM of aggregates of CR-treated Aβ_{1-40}. This material is available free of charge via the Internet at http://pubs.acs.org.

Author Information

Corresponding Author

*Corresponding authors. For E.G., e-mail emmanuelle.gothelid@fysik.uu.se; phone +46 18 471 3616. For P.I.A., e-mail Per.Arvidsson@biorg.uu.se, Per.Arvidsson@astrazeneca.com; phone +46-8 553 25923; fax +46-8 553 28877.

Author Contributions

Partha Pratim Bose, Urmimala Chatterjee, and Ling Xie performed the experimental work and data analysis. Per I Arvidsson, Emmanuelle Göthelid, and Jan Johansson provided guidance and advice. The manuscript was written through contributions of all authors.

Funding Sources

This work was supported by a grant from Stiftelsen Olle Engkvist Byggmästare and by the Swedish Research Council. E.G.D thanks the European Commission (FP6 grant # IST027017 NeuroProbes) and the Göran Gustafsson foundation for their support.

Abbreviations

AD, Alzheimer's disease; Aβ, amyloid β-peptides; AFM, Atomic force microscopy; CD, circular dichroism; CR, Congo red; HFIP, 1,1,1,3,3,3-hexafluoroisopropanol; PBS, phosphate-buffered saline; PICUP, photo-induced cross-linking of unmodified protein; SDS−PAGE, sodium dodecyl sulfate−polyacrylamide gel electrophoresis.

References

1. Chiti, F., and Dobson, C. M. (2006) Protein misfolding, functional amyloid, and human disease. *Annu. Rev. Biochem. 75*, 333–366.

2. Ecroyd, H., and Carver, J. A. (2008) Unraveling the mysteries of protein folding and misfolding. *IUBMB Life 60*, 769–774.

3. Soto, C., and Estrada, L. D. (2008) Protein misfolding and neurodegeneration. *Arch. Neurol. 65*, 184–189.

4. Roychaudhuri, R., Yang, M., Hoshi, M. M., and Teplow, D. B. (2009) Amyloid β-protein assembly and Alzheimer disease. *J. Biol. Chem. 284*, 4749–4753.

DOI: 10.1021/cn900041x | *ACS Chem. Neurosci.* (2010), *1*, 315–324

5. Adessi, C., Frossard, M. J., Boissard, C., Fraga, S., Bieler, S., Ruckle, T., Vilbois, F., Robinson, S. M., Mutter, M., Banks, W. A., and Soto, C. (2003) Pharmacological profiles of peptide drug candidates for the treatment of Alzheimer's disease. *J. Biol. Chem. 278*, 13905–13911.

6. Gong, Y., Chang, L., Viola, K. L., Lacor, P. N., Lambert, M. P., Finch, C. E., Krafft, G. A., and Klein, W. L. (2003) Alzheimer's disease-affected brain: Presence of oligomeric A beta ligands (ADDLs) suggests a molecular basis for reversible memory loss. *Proc. Natl. Acad. Sci. U.S.A. 100*, 10417–10422.

7. Gellermann, G. P., Byrnes, H., Striebinger, A., Ullrich, K., Mueller, R., Hillen, H., and Barghorn, S. (2008) Aβ-globulomers are formed independently of the fibril pathway. *Neurobiol. Dis. 30*, 212–220.

8. Kayed, R., Pensalfini, A., Margol, L., Sokolov, Y., Sarsoza, F., Head, E., Hall, J., and Glabe, C. (2009) Annular protofibrils are a structurally and functionally distinct type of amyloid oligomer. *J. Biol. Chem. 284*, 4230–4237.

9. Viola, K. L., Velasco, P. T., and Klein, W. L. (2008) Why Alzheimer's is a disease of memory: The attack on synapses by A beta oligomers (ADDLs). *J. Nutr., Health Aging 12*, 51S–57S.

10. Martins, I. C., Kuperstein, I., Wilkinson, H., Maes, E., Vanbrabant, M., Jonckheere, W., Van Gelder, P., Hartmann, D., D'Hooge, R., De Strooper, B., Schymkowitz, J., and Rousseau, F. (2008) Lipids revert inert Abeta amyloid fibrils to neurotoxic protofibrils that affect learning in mice. *EMBO J. 27*, 224–233.

11. Feng, Y., Wang, X. P., Yang, S. G., Wang, Y. J., Zhang, X., Du, X. T., Sun, X. X., Zhao, M., Huang, L., and Liu, R. T. (2009) Resveratrol inhibits beta-amyloid oligomeric cytotoxicity but does not prevent oligomer formation. *Neurotoxicology 30*, 986–995.

12. Bravo, R., Arimon, M., Valle-Delgado, J. J., Garcia, R., Durany, N., Castel, S., Cruz, M., Ventura, S., and Fernandez-Busquets, X. (2008) Sulfated polysaccharides promote the assembly of amyloid beta(1−42) peptide into stable fibrils of reduced cytotoxicity. *J. Biol. Chem. 283*, 32471–32483.

13. Necula, M., Breydo, L., Milton, S., Kayed, R., van der Veer, W. E., Tone, P., and Glabe, C. G. (2007) Methylene blue inhibits amyloid Aβ oligomerization by promoting fibrillization. *Biochemistry 46*, 8850–8860.

14. Ehrnhoefer, D. E., Bieschke, J., Boeddrich, A., Herbst, M., Masino, L., Lurz, R., Engemann, S., Pastore, A., and Wanker, E. E. (2008) EGCG redirects amyloidogenic polypeptides into unstructured, off-pathway oligomers. *Nat. Struct. Mol. Biol. 15*, 558–566.

15. Findeis, M. A. (2000) Approaches to discovery and characterization of inhibitors of amyloid beta-peptide polymerization. *Biochim. Biophys. Acta 1502*, 76–84.

16. Meinhardt, J., Sachse, C., Hortschansky, P., Grigorieff, N., and Fandrich, M. (2009) Abeta(1−40) fibril polymorphism implies diverse interaction patterns in amyloid fibrils. *J. Mol. Biol. 386*, 869–877.

17. Frid, P., Anisimov, S. V., and Popovic, N. (2007) Congo red and protein aggregation in neurodegenerative diseases. *Brain Res. Rev. 53*, 135–160.

18. Burgevin, M. C., Passat, M., Daniel, N., Capet, M., and Doble, A. (1994) Congo red protects against toxicity of beta-amyloid peptides on rat hippocampal neurones. *Neuroreport 5*, 2429–2432.

19. Gellermann, G. P., Ullrich, K., Tannert, A., Unger, C., Habicht, G., Sauter, S. R., Hortschansky, P., Horn, U., Mollmann, U., Decker, M., Lehmann, J., and Fandrich, M. (2006) Alzheimer-like plaque formation by human macrophages is reduced by fibrillation inhibitors and lovastatin. *J. Mol. Biol. 360*, 251–257.

20. Arimon, M., Diez-Perez, I., Kogan, M. J., Durany, N., Giralt, E., Sanz, F., and Fernandez-Busquets, X. (2005) Fine structure study of Abeta1−42 fibrillogenesis with atomic force microscopy. *FASEB J. 19*, 1344–1346.

21. Crowther, D. C., Kinghorn, K. J., Miranda, E., Page, R., Curry, J. A., Duthie, F. A., Gubb, D. C., and Lomas, D. A. (2005) Intraneuronal Abeta, non-amyloid aggregates and neurodegeneration in a *Drosophila* model of Alzheimer's disease. *Neuroscience 132*, 123–135.

22. Chander, H., Chauhan, A., and Chauhan, V. (2007) Binding of proteases to fibrillar amyloid-beta protein and its inhibition by Congo red. *J. Alzheimers Dis. 12*, 261–269.

23. Bose, M., Gestwicki, J. E., Devasthali, V., Crabtree, G. R., and Graef, I. A. (2005) 'Nature-inspired' drug-protein complexes as inhibitors of Abeta aggregation. *Biochem. Soc. Trans. 33*, 543–547.

24. Gestwicki, J. E., Crabtree, G. R., and Graef, I. A. (2004) Harnessing chaperones to generate small-molecule inhibitors of amyloid beta aggregation. *Science 306*, 865–869.

25. Fancy, D. A. (2000) Elucidation of protein-protein interactions using chemical cross-linking or label transfer techniques. *Curr. Opin. Chem. Biol. 4*, 28–33.

26. Bitan, G., Kirkitadze, M. D., Lomakin, A., Vollers, S. S., Benedek, G. B., and Teplow, D. B. (2003) Amyloid beta -protein (Abeta) assembly: Abeta 40 and Abeta 42 oligomerize through distinct pathways. *Proc. Natl. Acad. Sci. U.S.A. 100*, 330–335.

27. Bartolini, M., Bertucci, C., Bolognesi, M. L., Cavalli, A., Melchiorre, C., and Andrisano, V. (2007) Insight into the kinetic of amyloid beta (1−42) peptide self-aggregation: Elucidation of inhibitors' mechanism of action. *ChemBioChem 8*, 2152–2161.

28. Goldbeck, R. A., Thomas, Y. G., Chen, E., Esquerra, R. M., and Kliger, D. S. (1999) Multiple pathways on a protein-folding energy landscape: kinetic evidence. *Proc. Natl. Acad. Sci. U.S.A. 96*, 2782–2787.

29. Ono, K., Condron, M. M., Ho, L., Wang, J., Zhao, W., Pasinetti, G. M., and Teplow, D. B. (2008) Effects of grape seed-derived polyphenols on amyloid beta-protein self-assembly and cytotoxicity. *J. Biol. Chem. 283*, 32176–32187.

30. Pratim Bose, P., Chatterjee, U., Nerelius, C., Govender, T., Norström, T., Gogoll, A., Sandegren, A., Göthelid, E., Johansson, J., and Arvidsson, P. I. (2009) Poly-*N*-methylated amyloid β-Peptide (Aβ) C-terminal fragments reduce Aβ toxicity in vitro and in *Drosophila melanogaster*. *J. Med. Chem. 52*, 8002–8009.

31. Podlisny, M. B., Walsh, D. M., Amarante, P., Ostaszewski, B. L., Stimson, E. R., Maggio, J. E., Teplow, D. B., and Selkoe, D. J. (1998) Oligomerization of endogenous and synthetic

DOI: 10.1021/cn900041x | *ACS Chem. Neurosci.* (2010), *1*, 315–324

amyloid β-protein at nanomolar levels in cell culture and stabilization of monomer by Congo red. *Biochemistry 37*, 3602–3611.

32. Feng, B. Y., Toyama, B. H., Wille, H., Colby, D. W., Collins, S. R., May, B. C., Prusiner, S. B., Weissman, J., and Shoichet, B. K. (2008) Small-molecule aggregates inhibit amyloid polymerization. *Nat. Chem. Biol. 4*, 197–199.

33. McGovern, S. L., Caselli, E., Grigorieff, N., and Shoichet, B. K. (2002) A common mechanism underlying promiscuous inhibitors from virtual and high-throughput screening. *J. Med. Chem. 45*, 1712–1722.

34. Roterman, I., Król, M., Nowak, M., Konieczny, L., Rybarska, J., Stopa, B., Piekarska, B., and Zemanek, G. (2001) Why Congo red binding is specific for amyloid proteins - model studies and a computer analysis approach. *Med. Sci. Monit. 7*, 771–784.

35. Klunk, W. E., Debnath, M. L., and Pettegrew, J. W. (1994) Development of small molecule probes for the beta-amyloid protein of Alzheimer's disease. *Neurobiol. Aging 15*, 691–698.

36. Lockhart, A. (2006) Imaging Alzheimer's disease pathology: One target, many ligands. *Drug Discovery Today 11*, 1093–1099.

37. Ye, L., Morgenstern, J. L., Gee, A. D., Hong, G., Brown, J., and Lockhart, A. (2005) Delineation of positron emission tomography imaging agent binding sites on beta-amyloid peptide fibrils. *J. Biol. Chem. 280*, 23599–23604.

38. Lee, C. W., Zhuang, Z. P., Kung, M. P., Plossl, K., Skovronsky, D., Gur, T., Hou, C., Trojanowski, J. Q., Lee, V. M., and Kung, H. F. (2001) Isomerization of (*Z*,*Z*)- to (*E*,*E*)-1-bromo-2,5-bis-(3-hydroxycarbonyl-4-hydroxy)styryl-benzene in strong base: Probes for amyloid plaques in the brain. *J. Med. Chem. 44*, 2270–2275.

39. Styren, S. D., Hamilton, R. L., Styren, G. C., and Klunk, W. E. (2000) X-34, a fluorescent derivative of Congo red: A novel histochemical stain for Alzheimer's disease pathology. *J. Histochem. Cytochem. 48*, 1223–1232.

40. Klunk, W. E., Bacskai, B. J., Mathis, C. A., Kajdasz, S. T., McLellan, M. E., Frosch, M. P., Debnath, M. L., Holt, D. P., Wang, Y., and Hyman, B. T. (2002) Imaging Abeta plaques in living transgenic mice with multiphoton microscopy and methoxy-X04, a systemically administered Congo red derivative. *J. Neuropathol. Exp. Neurol. 61*, 797–805.

41. Walsh, D. M., Klyubin, I., Fadeeva, J. V., Cullen, W. K., Anwyl, R., Wolfe, M. S., Rowan, M. J., and Selkoe, D. J. (2002) Naturally secreted oligomers of amyloid beta protein potently inhibit hippocampal long-term potentiation in vivo. *Nature 416*, 535–539.

42. McLean, C. A., Cherny, R. A., Fraser, F. W., Fuller, S. J., Smith, M. J., Beyreuther, K., Bush, A. I., and Masters, C. L. (1999) Soluble pool of Abeta amyloid as a determinant of severity of neurodegeneration in Alzheimer's disease. *Ann. Neurol. 46*, 860–866.

43. Shankar, G. M., Li, S., Mehta, T. H., Garcia-Munoz, A., Shepardson, N. E., Smith, I., Brett, F. M., Farrell, M. A., Rowan, M. J., Lemere, C. A., Regan, C. M., Walsh, D. M., Sabatini, B. L., and Selkoe, D. J. (2008) Amyloid-beta protein dimers isolated directly from Alzheimer's brains impair synaptic plasticity and memory. *Nat. Med. 14*, 837–842.

44. Lorenzo, A., and Yankner, B. A. (1994) Beta-amyloid neurotoxicity requires fibril formation and is inhibited by congo red. *Proc. Natl. Acad. Sci. U.S.A. 91*, 12243–12247.

45. Pellarin, R., Guarnera, E., and Caflisch, A. (2007) Pathways and intermediates of amyloid fibril formation. *J. Mol. Biol. 374*, 917–924.

46. Hartley, D. M., Walsh, D. M., Ye, C. P., Diehl, T., Vasquez, S., Vassilev, P. M., Teplow, D. B., and Selkoe, D. J. (1999) Protofibrillar intermediates of amyloid beta-protein induce acute electrophysiological changes and progressive neurotoxicity in cortical neurons. *J. Neurosci. 19*, 8876–8884.

47. Cherny, I., and Gazit, E. (2008) Amyloids: Not only pathological agents but also ordered nanomaterials. *Angew. Chem., Int. Ed. 47*, 4062–4069.

48. Horcas, I., Fernandez, R., Gomez-Rodriguez, J. M., Colchero, J., Gomez-Herrero, J., and Baro, A. M. (2007) WSXM: A software for scanning probe microscopy and a tool for nanotechnology. *Rev. Sci. Instrum. 78*, 013705.

49. Towbin, H., Staehelin, T., and Gordon, J. (1979) Electrophoretic transfer of proteins from polyacrylamide gels to nitrocellulose sheets: procedure and some applications. *Proc. Natl. Acad. Sci. U.S.A. 76*, 4350–4354.

DOI: 10.1021/cn900041x | *ACS Chem. Neurosci.* (2010), *1*, 315–324